CHAPTER

2

Multilevel computational models for predicting the cellular effects of noninvasive brain stimulation

Asif Rahman, Belen Lafon, Marom Bikson[1]

Department of Biomedical Engineering, The City College of New York, CUNY, New York, NY, USA

[1]Corresponding author: Tel.: +212-650-6791; Fax: +212-650-6727, e-mail address: bikson@ccny.cuny.edu

Abstract

Since 2000, there has been rapid acceleration in the use of tDCS in both clinical and cognitive neuroscience research, encouraged by the simplicity of the technique (two electrodes and a battery powered stimulator) and the perception that tDCS protocols can be simply designed by placing the anode over the cortex to "excite," and the cathode over cortex to "inhibit." A specific and predictive understanding of tDCS needs experimental data to be placed into a quantitative framework. Biologically constrained computational models provide a useful framework within which to interpret results from empirical studies and generate novel, testable hypotheses. Although not without caveats, computational models provide a tool for exploring cognitive and brain processes, are amenable to quantitative analysis, and can inspire novel empirical work that might be difficult to intuit simply by examining experimental results. We approach modeling the effects of tDCS on neurons from multiple levels: modeling the electric field distribution, modeling single-compartment effects, and finally with multicompartment neuron models.

Keywords

Transcranial direct current stimulation, Computational neuroscience, Transcranial magnetic stimulation, Hodgkin–Huxley models, Numerical simulation

This chapter addresses the contribution of computational neuron models and basic animal research to our understanding of the neural mechanisms of transcranial direct current stimulation (tDCS). Though we attempt to put in perspective key computational studies to model experimental data in animals, our goal is not an exhaustive

Progress in Brain Research, Volume 222, ISSN 0079-6123, http://dx.doi.org/10.1016/bs.pbr.2015.09.003

cataloging of relevant computational or animal studies, but rather to put them in the context of ongoing effort to improve our understanding of tDCS. Similarly, though we point out essential features of meaningful studies, we refer readers to original work for methodological details.

Modern noninvasive brain stimulation techniques have their origin in decades-old theoretical and experimental applications of electrical stimulation on central and peripheral nervous tissue. Beginning with the demonstration of the electrical excitability of the cerebral cortex by Gustav Fritsch and Eduard Hitzig in 1870 (Carlson and Devinsky, 2009; Fritsch and Hitzig, 1870), the study of the nervous system has been intimately connected with the application of electricity to influence or evoke neural activity. While the electrical stimulation of nervous tissue has made remarkable contributions to neuroscience, the motivation behind tDCS is to modulate cellular activity to support cognitive, sensory, and motor functions (i.e., neuromodulation). The cellular basis of neuromodulation with direct current stimulation (DCS) remains an active area of research with evidence from both *in vitro* and *in vivo* animal models of tDCS. The motivation for both animal research and computational modeling of tDCS is evident: to allow rapid and risk-free screening of stimulation protocols and to address the mechanisms of tDCS with the ultimate goal of informing clinical tDCS efficacy and safety. This chapter highlights some of the known mechanisms of tDCS with an emphasis on developing a predictive understanding of DCS through multilevel computational neuron models. We present the known cellular mechanisms of tDCS derived from experimental and theoretical analysis beginning with the basic question: which neural elements are excited by DCS?

1 WHICH NEURAL ELEMENTS ARE EXCITED BY DIRECT CURRENT STIMULATION?

A battery-driven constant current generator delivering weak currents ($\leq$1 mA) between a pair of saline-soaked sponge electrodes induces a voltage gradient (change in voltage/change in distance) in the brain (Fig. 1; Miranda et al., 2007a; Rahman et al., 2013; Ranck, 1975). The direct effect of the induced electric field is a passive change in membrane potential (V_m) (Chan and Nicholson, 1986; Radman et al., 2009b; Tranchina and Nicholson, 1986). The timing and magnitude of a change in V_m is determined by the resistive and capacitive properties of the cellular membrane. A neuron in a resistive extracellular media can be modeled as a series of equivalent electrical circuits (compartments) coupled together with an internal resistance (R_i) (Gerstner et al., 1997; Holt and Koch, 1999). The extracellular voltage (V_e) compartment specifically polarizes the cell (Arlotti et al., 2012; Chan et al., 1988; Rahman et al., 2013). That is, current entering cellular compartments near the positive electrode hyperpolarizes the membrane (membrane potential becomes more negative), while current flowing out of compartments proximal to the negative electrode is depolarized (membrane potential becomes more positive) (Chan and Nicholson, 1986; Chan et al., 1988; Durand and Bikson, 2001; Radman et al., 2009b). For typical cortical pyramidal cells in layer 5, a positive electrode on the

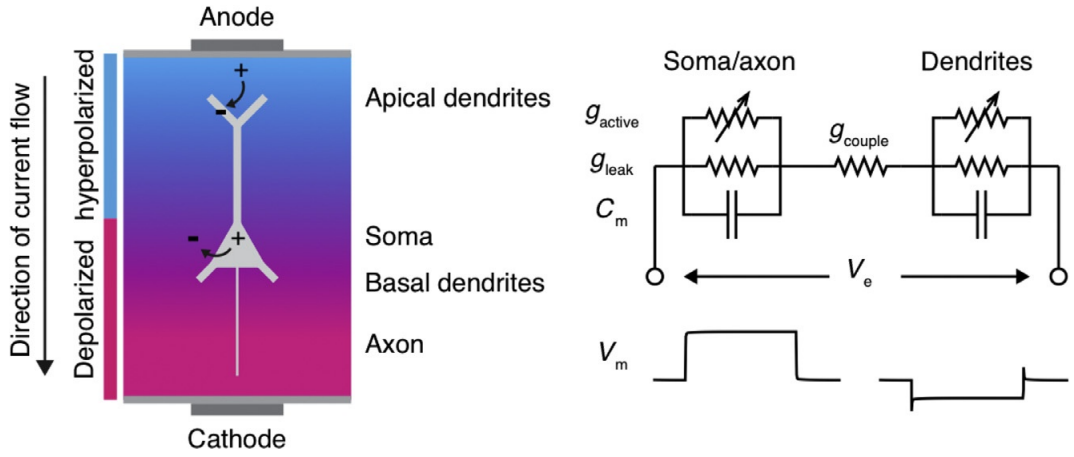

FIGURE 1

Cortical pyramidal cells are biphasically polarized in the voltage gradient induced by tDCS. Compartments proximal to the anode are hyperpolarized, while distal compartments are simultaneously depolarized. A simple two-compartment model is simulated to show the relative biphasic polarization in the soma/axon compartment and dendritic compartments.

cortical surface (referred to as the anode) hyperpolarizes apical dendrites while simultaneously depolarizing the soma and basal dendrites (Fig. 1).

The passive change in membrane potential alters current flow through voltage-gated ion channels (Ali et al., 2013; Bikson et al., 1999; Stagg and Nitsche, 2011). The magnitude and timing of these currents depend on channel gating kinetics. Sodium and potassium channels in the soma, responsible for action potential generation, are especially susceptible to changes in voltage when the somatic membrane potential is depolarized or hyperpolarized by DCS (Bikson et al., 2004). The site of action potential initiation, the axon initial segment, may be especially susceptible to somatic membrane potential changes because of the high density of sodium channels. Recently, other important voltage-dependent channels have been identified that play a critical role in activating neurons, including the HCN channel (Ali et al., 2013).

All neural elements, including dendrites, somas, and axons, are susceptible to polarization in the induced electric field to different magnitudes depending on passive and active membrane properties and the orientation of the neuron relative to the direction of current flow. In the simplest case of a cylindrical axon of semi-infinite length in a homogenous extracellular media exposed to a uniform electric field, current flows from the positive electrode to the negative electrode resulting in polarization along the longitudinal axis (Fig. 2; Ranck, 1975; Rattay, 1989).

2 MODELING ELECTRICAL STIMULATION

Modeling electrical stimulation of neural elements can be performed as a combination of two steps. The first step involves calculation of the spatial distributions of the induced electric fields produced by tDCS (Datta et al., 2009; Miranda et al., 2006).

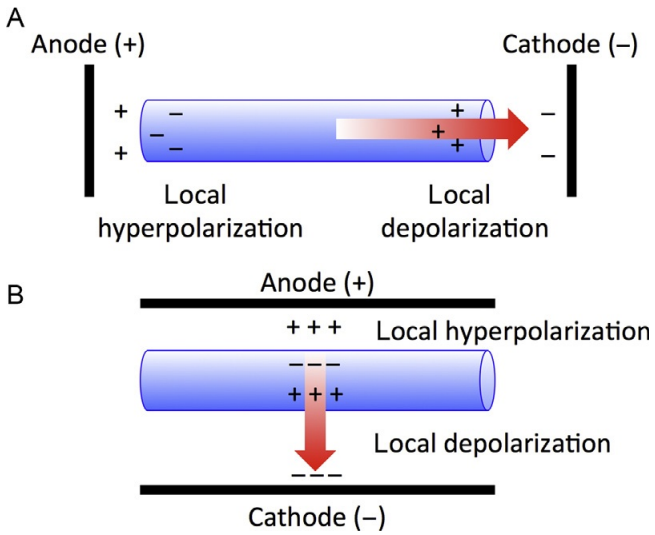

FIGURE 2

Polarization along a fiber modeled as a cylinder with parallel electrodes. (A) Current flows from the positive electrode (anode) to the negative electrode (cathode). A fiber oriented along the direct of current flow is maximally hyperpolarized near the anode and maximally depolarized near the cathode. (B) Fibers oriented perpendicular to the direct of current flow are not polarized by the induced electric field since their diameter is small enough for the internal charge distribution to be negligible.

This is achieved by using finite element models of current flow (Fig. 3A). Since tDCS generates static electric fields at 0 Hz (direct current), it is unnecessary to perform calculations of the temporal distributions of the induced field (calculations are at steady state). The second step is to model the polarization neuronal structures using compartmental analysis.

On the macroscopic scale, tissue resistivity and cerebrospinal fluid influence current flow, electric field direction, and magnitude (Miranda et al., 2007a,b; Salvador et al., 2010). White matter, which is anisotropic (electrical conductivity of brain tissue is inhomogeneous), results in a gyri-specific spatial distribution of the electric field (Miranda et al., 2007a,b; Salvador et al., 2010), which has some important functional consequences for neural excitability. Simply stated, the change in membrane potential along axons is highly influenced by tissue heterogeneity between gray and white matter. Modeling work shows that changes in tissue conductivity can give rise to action potentials in a myelinated axon (Miranda et al., 2007a). Many models of cellular polarization in an electric field, however, implicitly utilize the "quasi-uniform" assumption, which allows one to consider a uniform electric field along a cell without considering tissue conductivity (Bikson et al., 2012).

Salvador et al. (2011) considered how the electric field-induced polarization (field generated by a transcranial magnetic stimulation coil) changes along the axon as a function of tissue inhomogeneity and cortical geometry by modeling bent axons originating in the gray matter (either in the gyral crown or wall) and projecting down

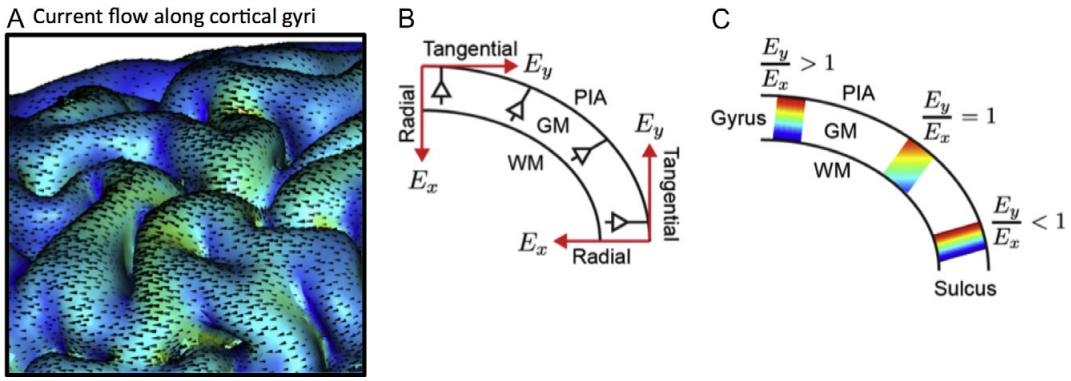

FIGURE 3

tDCS produces current flow along cortical gyri. (A) Finite element models of current flow illustrate the directionality of the net electric field. (B) The net electric field can be decomposed into a tangential (E_y) and radial (E_x) vector components. The relative magnitude of these vectors determines the direction of net current flow. (C) The relative electric field magnitude at the gyral wall is typically >1, suggesting tangential current flow dominates in the gyral crown. Models suggest pyramidal cells in the gyral crown that are oriented orthogonal to the tangential electric field may not be polarized. Processes that are oriented along the tangential field in the gyral crown, like axons, are polarized. In the gyral wall, the dominant electric field direction is inward (radial). Current flows along neurons in the gyral wall and polarizes the cell along its somatodendritic axis.

to subcortical regions (Salvador et al., 2010, 2011). Polarization was maximal at the site of axonal bends, consistent with previous modeling studies in strong (like TMS) and weak (like tDCS) electric fields (BeMent and Ranck, 1969; Plonsey and Barr, 2000; Ranck, 1975; Rubinstein, 1993).

There is a lack of polarization along the somatodendritic axis when a tangential field is directed perpendicular to a pyramidal neuron (Fig. 2; Bikson et al., 2004; Rahman et al., 2013). However, a straight axon, branching off the main axon, oriented parallel to the electric field polarized maximally at the terminal and an action potential was generated near the terminal, which propagates antidromically toward the main axon (Arlotti et al., 2012; Hause, 1975; Rahman et al., 2013). This is consistent with previously reported findings that the electric field direction may preferentially polarize alternate neural processes to the soma (like axon terminals and fiber bending points) to induce APs independent of somatic polarization (Hause, 1975; Plonsey and Barr, 2000; Ranck, 1975; Rubinstein, 1993). It should be noted that the field strength in the Salvador model was simulated for TMS, which is significantly higher than tDCS-induced fields, but qualitatively it demonstrates the concept of axon terminal polarization by tangential fields in gyral crowns. Recent analysis of the distribution of tangential and radial electric field components in the gyral crown and wall shows that tangential direct electric fields do dominate in gyral crowns (Rahman et al., 2013). Processes along the direction of the electric field in regions where tangential electric fields dominate are therefore subject to greater polarization than processes oriented orthogonal to the electric field.

Since cortical convolutions influence electric field direction, recent studies have looked closely at the direction of the induced electric field in gyral crowns and walls. The direction of the extracellular voltage gradient in the gyrus is qualitatively different from the gyral walls (Fig. 3A, false color represents the calculated voltage gradient in a finite element model of current flow in a gyri-precise head model of tDCS). The induced electric field is decomposed into two field components (Fig. 3B). The radial component is directed perpendicular to the cortical surface (parallel to the somatodendritic axis of cortical pyramidal neurons). The tangential field is parallel to the cortical surface (perpendicular to the somatodendritic axis of pyramidal neurons). The direction of the induced electric field relative to the neuron has important functional significance (discussed in the next sections). By analyzing the electric field directions regionally under electrodes, and in gyral crowns and walls, Rahman et al. (2013) found tangential fields are 7–12 times more prevalent than radial fields in the gyral crown and 0.3–2 times more prevalent in gyral walls. The importance of this finding is that electric fields are dominantly oriented along corticocortical afferent axons and not along the somatodendritic axis in the gyral crown.

The relative magnitude of the two components of the induced electric field (E_x = normal and E_y = tangential) is considered and quantified on multiple scales (Fig. 3B), including global field distributions in the brain, regionally under/between electrodes, and in subregions on gyral crowns/walls. The ratio of tangential to normal (E_y/E_x) field magnitudes describes the relative magnitudes in each region, such that $E_y/E_x > 1$ corresponds to greater tangential fields on average and $E_y/E_x < 1$ corresponds to greater radial fields on average (Fig. 3C). The metric is represented in Fig. 3C with a schematic representation of the voltage distribution overlaid on each region of interest along a cortical gyrus.

Implicit to the current flow modeling described above and then to the neuronal polarization model described next is the quasi-uniform assumption. The quasi-uniform assumption suggests that for tDCS, the resulting electric fields produce a regional polarization that is well approximating by considering the uniform electric field in each region. Or put differently, during tDCS the small change in electric field over the scale of the neuronal axis can be modeled as uniform (Bikson et al., 2012).

3 QUANTIFYING MEMBRANE POLARIZATION

In the 1980s, Chan and colleagues (Chan and Nicholson, 1986; Chan et al., 1988) used electrophysiological recordings from turtle cerebellum and analytical modeling to quantify polarization under low-frequency sinusoid electric fields—these seminal studies identified morphological determinants of neuron sensitivity to applied electric fields. Bikson et al. (2004) extended this work to rat hippocampal CA1 neurons and then to cortical neurons (Radman et al., 2009a,b) with the approach of quantifying cell-specific polarization by weak DC fields using a single number—the "coupling constant" (also called the "coupling strength" or "polarization length").

Assuming that for weak electric fields (stimulation intensities too weak to significantly activate voltage-gated membrane channels, and well below action potential threshold), the resulting membrane polarization at any given compartment, including the soma, is linear with stimulation intensity. For uniform electric fields, the membrane polarization can be expressed as: $V_{tm} = \lambda * E$, where V_{tm} is the polarization of the compartment of interest (in: V), λ is the coupling constant (in: V per V/m, or simply: m), and E is the electric field (in: V/m) along the primary dendritic axis. For rat hippocampus and cortical neurons, the somatic coupling constant is in the range of 0.1–0.3 mV polarization per V/m electric field (Fig. 4; Bikson et al., 2004; Deans et al., 2007; Radman et al., 2009b). For ferret cortical neurons, the coupling is similarly ~0.25 mV per V/m (Fröhlich and McCormick, 2010). For humans, assuming scaling of sensitivity with total neuronal length (Joucla and Yvert, 2009, 2011), somatic depolarization per V/m might be higher than in animals.

The maximal depolarization occurs when the electric field is parallel with the somatodendritic axis, which corresponds to an electric field radial to the cortical surface (Hause, 1975; Rattay, 1989). Electric field orthogonal to the somatodendritic axis does not produce significant somatic polarization (Bikson et al., 2004; Chan et al., 1988). The somatic coupling strength is roughly related to the size of the cell and the dendritic asymmetry around the soma (Radman et al., 2009a; Svirskis et al.,

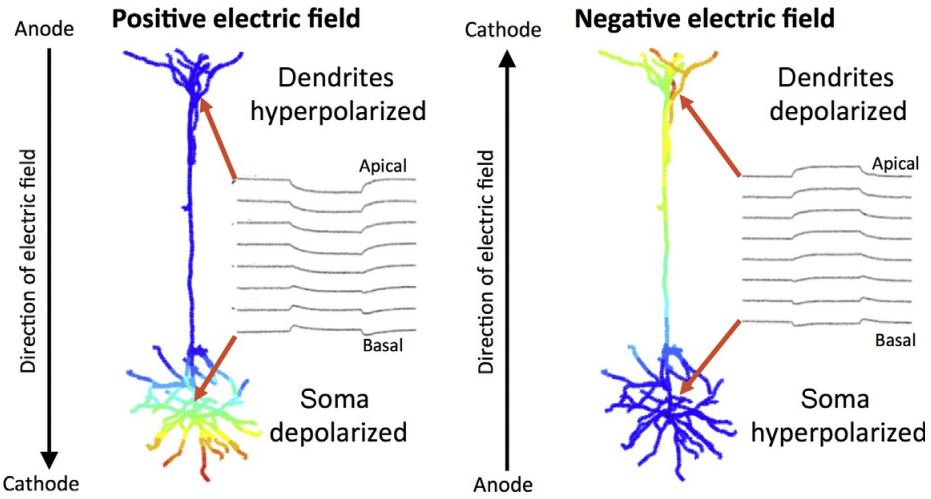

FIGURE 4

Compartment-specific polarization in a 3D reconstructed neuron. Simulation results from a 3D reconstructed neuron embedded in a resistive media and exposed to a uniform extracellular electric field oriented along the principal axis. Experimental results from voltage dye imaging (Bikson et al., 2004) are embedded next to the neurons to demonstrate how membrane potential changes along the cell in a multicompartment model. Compartments near the positive electrode are hyperpolarized (membrane potential is more negative, relative to the resting potential) and compartments are more depolarized (positive membrane potential relative to resting potential). The false color represents maximum (red (gray in the print version), depolarization) to minimum (blue (dark gray in the print version), hyperpolarization) polarization.

1997, 2001), making pyramidal neurons relatively sensitive. For cortical pyramidal neurons, the typical polarity of somatic polarization is consistent with the "somatic doctrine" (e.g., positive somatic depolarization for positive electric field). The polarity of the coupling constant is inverted for CA1 pyramidal neurons due to their inverted morphology. Using experimental and modeling techniques, the coupling constant of dendritic compartments can also be investigated; generally, the maximal polarization is expected at dendritic tufts and axon terminals (Bikson et al., 2004), but should not exceed, in animals, ~1 mV polarization per V/m electric field (Chan et al., 1988; Radman et al., 2007, 2009b).

In a computational analysis of axon terminal polarization in morphologically reconstructed cortical pyramidal neurons, Rahman et al. (2013) reported the terminal coupling constant is 2–3 times greater than soma-coupling constant, which is consistent to a similar analysis by Hause (1975). This finding suggests that axon terminals are more susceptible to polarization than somas. The terminal coupling constant is equivalent to the membrane length constant (λ, mm). The value of λ, which is proportional to the diameter of a segment of a neuron, determines the shape of voltage decay along a neuron. In our model, the length constant was uniform throughout the neuron. However, since axon diameter is not constant, the value of λ changes at every branch point and the approximation may be overestimating the polarization.

If tDCS produces a peak electric field of 0.3 V/m at 1 mA (with the majority of cortex at reduced values), then the maximal somatic polarization for the most sensitive cells is ~0.1 mV. Similarly, for 2 mA tDCS stimulation, the most sensitive cells in the brain region with the highest electric field would have somatic polarization of ~0.2 mV. Far from "closing the book" on tDCS mechanism, work by our group and others quantifying the sensitivity of neuron to weak DC fields has raised questions about how such minimal polarization could result in functional/clinical changes especially considering that endogenous "background" synaptic noise can exceed these levels. In recent years, motivated by increased evidence that transcranial stimulation with weak currents has functional effects, as well as ongoing questions about the role of endogenous electric fields which can have comparable electric fields, the mechanisms of amplification have been explored in animal studies; we organize these efforts by nonlinear single-cell properties.

4 POLARIZATION PROFILE OF A NEURON IN A UNIFORM ELECTRIC FIELD

Neurons exposed to a uniform electric field are compartment-specifically polarized. The magnitude of polarization in a compartment is a function of the polarization in neighboring compartments and the distance from the positive electrode (Rahman et al., 2013; Rattay, 1989). As current travels from the positive to the negative field electrode, a typical pyramidal cell is entirely polarized with compartments proximal to the positive electrode more hyperpolarized than the compartments proximal to the negative electrode. Compartments in the middle are also polarized but to a lesser

degree—therefore, a gradient of polarization exists along the cell in the direction of current flow. There is, theoretically, zero or negligible polarization at the midpoint of the cell (Fig. 4).

5 CABLE THEORY FORMULATION

The membrane polarization for a passive neuron exposed to an extracellular electric field can be estimated using a cable theoretic approach—by modeling each compartment as an equivalent electrical circuit embedded in a resistive media (Koch, 1984; Rall, 1959; Roth, 1994). The change in membrane potential along a straight fiber, expressed as the first spatial derivative, can be estimated using cable theory, which relates the change in V_m with the change in the extracellular voltage. Therein, knowing the extracellular voltage can provide an estimate of the approximate membrane potential in a compartment

$$\frac{\partial V_m}{\partial t} + \frac{\partial^2 V_m(x)}{\partial x^2} - V_m = \lambda^2 \frac{\partial^2 V_e(x)}{\partial x^2}. \tag{1}$$

The effect of extracellular stimulation on a uniform fiber can be formalized using the continuous cable equation (McNeal, 1976; Richardson et al., 2000). For uniform electric fields applied to a finite-length straight fiber, the activating function is zero along the membrane except at the ends. The activating function (represented by the right hand side of Eq. 1) describes the membrane potential as the second spatial derivative along the neuron (Eq. 2)

$$V_m(x) \propto \mathrm{AF} = \lambda^2 \frac{\partial^2 V_e(x)}{\partial x^2}. \tag{2}$$

The activating function is zero along the cell membrane except at the ends for uniform electric fields applied to a finite-length straight fiber (Eq. 3). In this case, a simple analytical solution exists relating the polarization at fiber terminals with the membrane length constant and the length of the fiber. Considering the electric field is in the same direction of the fiber, for $L < \lambda$ (where L is the physical length of the cable) the terminal polarization in steady-state conditions is $\pm E^* L/2$. For length $L > 4\lambda$, the terminal polarization is $\pm E\lambda$. This is valid for sealed-end boundary conditions ($\frac{\partial V_i(x)}{\partial x} = 0, x = 0, x = L$)

$$\lambda^2 \frac{\partial^2 V_e(x)}{\partial x^2} = \lambda^2 \frac{\partial^2 (E \cdot x)}{\partial x^2}. \tag{3}$$

For neurons (axons) with increased morphological and biophysical details (compartment diameter, membrane conductance), the polarization solution quickly increases the problem complexity, as it is necessary to consider the polarization of each compartment and then the axial currents such that for "realistic" cases we have no analytical solutions.

Perhaps the best example of approximating the steady-state V_m from V_e appears in the work of Joucla and Yvert (2009) which proposes the "mirror estimate." The mirror estimate has shown to be a good predictor of the steady-state membrane polarization under the effect of external electric fields for compact structures (Arlotti et al., 2012; Joucla and Yvert, 2011). The mirror estimate suggests that the membrane polarization V_m at fiber location x is simply the opposite of the extracellular potential V_e at that location. Using this steady-state solution, it becomes very simple to predict the membrane compartments and amplitudes of depolarization and hyperpolarization along the fiber or a complex neuron, since we only need to know the extracellular field distribution and not the second derivatives along the different directions of the cells dendritic tree. The mirror estimate predicts that regions located close to the cathode are depolarized, while regions located further away are hyperpolarized (Arlotti et al., 2012; Joucla et al., 2009). Unlike the activating function above, the mirror estimate only requires knowledge of the extracellular voltage gradient and not the membrane properties.

6 MODELING BIPHASIC POLARIZATION DURING DCS IN HODGKIN–HUXLEY-BASED NEURONS

Pyramidal cells exposed to an electric field polarize neuronal compartments along the direction of current flow. While the soma is typically the site of action potential initiation and the apical dendrites typically receive synaptic inputs, this biphasic polarization presents an interesting confounder for interpreting the effects of DCS. Somatic depolarization may increase the probability of firing an action potential but neurons are embedded in a network and receive synaptic inputs from thousands of presynaptic cells. Dendritic polarization may change the synaptic input ($I_{syn} = g_{syn}*(E_{syn} - V_m)$) because the synaptic current flow across an excitatory AMPA synapse is a function of the membrane potential. The change in synaptic drive ($E_{syn} - V_m$) during DCS therefore directly modulates synaptic current flow.

Recently, simple two-compartment models have been used to account for the biphasic polarization. According to a two-compartment model, the cell consists of one proximal compartment, usually representing the basal dendrites, soma and axon; and a distal compartment including apical dendrites. Many interesting computational effects probably rely on the interaction between them, thus providing an essential tool for a better understanding of the effects of extracellular fields on neuronal activity. Moreover, two-compartment models can also work as the structural basis of a neural network to study more complex behaviors, such as synchronization. Park et al. (2005) implemented a quasi-unidimensional neural network model to understand how applied electric fields can modulate firing time and phase synchronization (Park et al., 2005). Each neuron was modeled as a Pinsky–Rinzel two-compartment neuron consisting of a dendrite and a soma compartment separated by a conductance g_c (Pinsky and Rinzel, 1994).

Building on the Pinsky–Rinzel model, Park et al. (2005) proposed that an extracellular electric field effect can be modeled by the current that flows between the two compartments of the neuron as $I_{DS} = g_c\,(V_d - V_s)$. Where $(V_d - V_s)$ is the difference between the *intracellular* voltage in the somatic and the dendritic chamber, and g_c is the conductance between the two compartments. Embedding these neurons in a resistive array, they were able to make testable predictions such as polarity and intensity of electric field needed to synchronize the neural network. Using a more simplistic approach, Yi et al. (2014a,b) analyzed the dynamical states of a single neuron using a modified Morris–Lecar model as proposed in Prescott et al. (2008) and Yi et al. (2014b). In their two-compartment model, the cell is described by the somatic compartment which contains Na^+ and K^+ conductances responsible for action potential generation and is connected to the dendritic compartment by a coupling conductance g_c. In order to facilitate the dynamical analysis, the dendritic compartment includes only a passive conductance. The membrane potential dynamics for each compartment are set by the following set of equations:

$$-C_m\frac{dV_s}{dt} = \acute{g}_{Na}m_\infty(V_s)(V_s - E_{Na}) + \acute{g}_K w(V_s - E_K) + g_{sl}(V_s - E_{sl}) - \frac{g_c}{p}(V_d + V_E - V_s) \tag{4}$$

$$-C_m\frac{dV_d}{dt} = g_{dl}(V_d - E_{dl}) + g_c(V_d + V_E - V_s). \tag{5}$$

The uniform extracellular electric field is modeled in a similar way to that in Park et al. (2005). The factors p and $(1-p)$ account for the relative area occupied by the soma and dendrites. Using this approach, Yi et al. (2014a,b) described the dynamical states of a two-compartment neuron under electric fields predicting the intensity of electric field necessary to induce spiking activity. In a later study, the same group described how the biophysical bases of spike initiation dynamics are affected by electric fields (Yi et al., 2014a).

7 AXON TERMINAL POLARIZATION

There are two complementary approaches to model the polarization of axon terminals (Arlotti et al., 2012): (1) to estimate polarization coupling from the soma and (2) to directly consider polarization of the terminus. Cable theory predicts the voltage decay along a semi-infinite axon as $\Delta V(x) = V_0 e^{-x/\lambda}$ (BeMent and Ranck, 1969; Plonsey and Barr, 2000; Rall, 2011; Ranck, 1975). However, this simplified passive case does not hold true during activity. Recent experimental evidence shows that somatic depolarization broadens the AP width, which indicates that action potentials are not mere digital signaling devices but behave as analog devices with graded signaling (Sasaki et al., 2012; Shu et al., 2006). Sasaki et al. (2012) depolarized pyramidal somas and measured activity at presynaptic terminals during an action

potential. Synaptic terminals at axons arborized near the soma (like in the hippocampus) experienced increased calcium influx when the soma-depolarized AP (broadened AP) innervated the terminal. In their analysis, Sasaki et al. found that for terminals close to the soma (effective distance from soma along axon within 100 μm), there was an increase in presynaptic calcium influx but for terminals >300 μm or more than two branch points from the soma there was no significant increase in calcium influx. This important experimental evidence shows that somatic polarization independent of axon terminal polarization can change synaptic output, for terminals near the soma, by changing the AP shape.

Recent studies have shown that axon terminals are in fact 2–3 times more sensitive than pyramidal somas. For a straight fiber of semi-infinite length, the maximal polarization at the terminal is $V_t = E\lambda\cos(\theta)$. An analytical solution to the cable equation shows that for bent axons the terminal polarization is coupled with the polarization at the last bend point: $V_t = E\lambda\cos(\theta)\tanh\left(\frac{L}{\lambda}\right) + V_o/\cosh\left(\frac{L}{\lambda}\right)$. Note that by assuming the voltage at the last branch point V_o is 0 and the terminal is very far from the last branch point ($\tanh(L/\lambda) = 1$), we arrive at the approximation for a straight fiber where the terminal polarization is a function of the electric field magnitude, the membrane length constant, and the angle relative to the electric field direction: $V_t = E\lambda\cos(\theta)$. Axonal polarization may play an important role in synaptic transmission. Experimental evidence has shown that DCS along fibers can polarize axons in cortical brain slices and modulate synaptic efficacy (Kabakov et al., 2012; Rahman et al., 2013).

8 A QUANTITATIVE FRAMEWORK FOR PREDICTING NEURONAL VOLTAGE OUTPUT

Based on the experimental evidence that DCS modifies synaptic efficacy, we propose a quantitative framework for evaluating the voltage output during dynamic synaptic transmission. The neuronal population response (Eq. 6) to excitatory presynaptic drive can be modeled as the averaged voltage response $V(t)$ (Richardson et al., 2005). A train of presynaptic spikes arriving down input fiber n over a large population of N_f input fibers at time t evokes excitatory postsynaptic potentials $\alpha(t)$

$$V(t) = \sum_{n=1}^{N_f} \sum_{\{t_{nk}\}} A_k \alpha(t - t_k). \tag{6}$$

In the above modeling framework, the electric field effect on synaptic efficacy (A_k), the effect on the number of synchronously active inputs (N_f), and the change in timing of inputs by electric fields can be directly modeled. Synaptic efficacy is

modulated by ~1.1%/V/m in the cortex and hippocampus (Bikson et al., 2004; Islam et al., 1997; Jefferys, 1981; Rahman et al., 2013). Incorporating this change in A_k yields an increase in the voltage output. Similarly, electric fields have been shown to change neuronal firing rate and thus may affect the timing and number of inputs, which our proposed model captures in t_{nk} and N_f.

9 NUMERICAL METHODS

Numerical solutions to the differential equations governing membrane potential and synaptic dynamics are solved using an exponential Euler integration scheme. This scheme is applicable for the neuron models employed here as all differential equations have the form:

$$\frac{dy}{dt} = A(t) - B(t)y \tag{7}$$

The solution at a time $t + dt$ is approximated in terms of the solution at time t by:

$$y(t+dt) = y(t)e^{-B(t)dt} + \frac{A(t)}{B(t)}\left(1 - e^{-B(t)dt}\right) \tag{8}$$

10 CONCLUSION

Computational neuron models provide a powerful research tool to test new tDCS protocols and explore biological processes. The level of description in a neuron model depends on the question being asked. All modeling approaches, however, must first estimate the induced electric field in the brain. The choice of describing a neuron as a single compartment with passive conductances or a multicompartmental model with active conductances requires careful consideration of the coupling between the extracellular electric field and the channel kinetics. We highlight some practical considerations in different modeling approaches but ultimately models should be informed-by and inform cellular mechanisms for animal experiments.

ACKNOWLEDGMENT/CONFLICT OF INTEREST

Support for this review comes from the Department of Defense (Air Force Office of Scientific Research), The Wallace Coulter Foundation, The Epilepsy Foundation, The Andy Grove Fund, and NIH. M.B. has equity in Soterix Medical Inc. The City University of New York has patents on brain stimulation with M.B. as inventor.

REFERENCES

Ali, M.M., Sellers, K.K., Frohlich, F., 2013. Transcranial alternating current stimulation modulates large-scale cortical network activity by network resonance. J. Neurosci. 33, 11262–11275.

Arlotti, M., Rahman, A., Minhas, P., Bikson, M., 2012. Axon terminal polarization induced by weak uniform DC electric fields: a modeling study. Conf. Proc. IEEE Eng. Med. Biol. Soc. 2012, 4575–4578.

BeMent, S.L., Ranck Jr., J.B., 1969. A quantitative study of electrical stimulation of central myelinated fibers. Exp. Neurol. 24, 147–170.

Bikson, M., Ghai, R.S., Baraban, S.C., Durand, D.M., 1999. Modulation of burst frequency, duration, and amplitude in the zero-Ca(2+) model of epileptiform activity. J. Neurophysiol. 82, 2262–2270.

Bikson, M., Inoue, M., Akiyama, H., Deans, J.K., Fox, J.E., Miyakawa, H., et al., 2004. Effects of uniform extracellular DC electric fields on excitability in rat hippocampal slices in vitro. J. Physiol. 557, 175–190.

Bikson, M., Dmochowski, J., Rahman, A., 2012. The "quasi-uniform" assumption in animal and computational models of non-invasive electrical stimulation. Brain Stimul. 6(4), 704–705.

Carlson, C., Devinsky, O., 2009. The excitable cerebral cortex Fritsch G, Hitzig E. Uber die elektrische Erregbarkeit des Grosshirns. Arch Anat Physiol Wissen 1870;37:300-32. Epilepsy Behav. 15, 131–132.

Chan, C.Y., Nicholson, C., 1986. Modulation by applied electric fields of Purkinje and stellate cell activity in the isolated turtle cerebellum. J. Physiol. 371, 89–114.

Chan, C.Y., Hounsgaard, J., Nicholson, C., 1988. Effects of electric fields on transmembrane potential and excitability of turtle cerebellar Purkinje cells in vitro. J. Physiol. 402, 751–771.

Datta, A., Bansal, V., Diaz, J., Patel, J., Reato, D., Bikson, M., 2009. Gyri-precise head model of transcranial direct current stimulation: improved spatial focality using a ring electrode versus conventional rectangular pad. Brain Stimul. 2, 201–207.

Deans, J.K., Powell, A.D., Jefferys, J.G., 2007. Sensitivity of coherent oscillations in rat hippocampus to AC electric fields. J. Physiol. 583, 555–565.

Durand, D.M., Bikson, M., 2001. Suppression and control of epileptiform activity by electrical stimulation: a review. Proc. IEEE 89, 1065–1082.

Fritsch, G.T., Hitzig, E., 1870. On the electrical excitability of the cerebrum. (G. Von Bonin, Trans.) (1960) In: Some Papers on the Cerebral Cortex. Charles C. Thomas, Springfield, IL.

Fröhlich, F., McCormick, D.A., 2010. Endogenous electric fields may guide neocortical network activity. Neuron 67, 129–143.

Gerstner, W., Kreiter, A.K., Markram, H., Herz, A.V., 1997. Neural codes: firing rates and beyond. Proc. Natl. Acad. Sci. U.S.A. 94, 12740–12741.

Hause, L., 1975. A mathematical model for transmembrane potentials secondary to extracellular fields. In: Sances, J., Larson, S. (Eds.), Electroanaesthesia: Biomedical and Biophysical Studies. Academic Press, New York.

Holt, G.R., Koch, C., 1999. Electrical interactions via the extracellular potential near cell bodies. J. Comput. Neurosci. 6, 169–184.

Islam, N., Aftabuddin, M., Moriwaki, A., Hori, Y., 1997. Effects of anodal polarization on protein kinase Cgamma (PKCgamma) in the rat brain. Indian J. Physiol. Pharmacol. 41, 204–210.

Jefferys, J.G.R., 1981. Influence of electric fields on the excitability of granule cells in guinea-pig hippocampal slices. J. Physiol. 319, 143–152.
Joucla, S., Yvert, B., 2009. The "mirror" estimate: an intuitive predictor of membrane polarization during extracellular stimulation. Biophys. J. 96, 3495–3508.
Joucla, S., Yvert, B., 2011. Modeling extracellular electrical neural stimulation: from basic understanding to MEA-based applications. J. Physiol. Paris 106, 146–158.
Kabakov, A.Y., Muller, P.A., Pascual-Leone, A., Jensen, F.E., Rotenberg, A., 2012. Contribution of axonal orientation to pathway-dependent modulation of excitatory transmission by direct current stimulation in isolated rat hippocampus. J. Neurophysiol. 107, 1881–1889.
Koch, C., 1984. Cable theory in neurons with active, linearized membranes. Biol. Cybern. 50, 15–33.
McNeal, D.R., 1976. Analysis of a model for excitation of myelinated nerve. IEEE Trans. Biomed. Eng. 23, 329–337.
Miranda, P.C., Lomarev, M., Hallett, M., 2006. Modeling the current distribution during transcranial direct current stimulation. Clin. Neurophysiol. 117, 1623–1629.
Miranda, P.C., Correia, L., Salvador, R., Basser, P.J., 2007a. The role of tissue heterogeneity in neural stimulation by applied electric fields. Conf. Proc. IEEE Eng. Med. Biol. Soc. 2007, 1715–1718.
Miranda, P.C., Correia, L., Salvador, R., Basser, P.J., 2007b. Tissue heterogeneity as a mechanism for localized neural stimulation by applied electric fields. Phys. Med. Biol. 52, 5603–5617.
Park, E.H., Barreto, E., Gluckman, B.J., Schiff, S.J., So, P., 2005. A model of the effects of applied electric fields on neuronal synchronization. J. Comput. Neurosci. 19, 53–70.
Pinsky, P.F., Rinzel, J., 1994. Intrinsic and network rhythmogenesis in a reduced Traub model for CA3 neurons. J. Comput. Neurosci. 1, 39–60.
Plonsey, R., Barr, R.C., 2000. Bioelectricity: A Quantitative Approach. Springer, New York, US.
Prescott, S.A., De Koninck, Y., Sejnowski, T.J., 2008. Biophysical basis for three distinct dynamical mechanisms of action potential initiation. PLoS Comput. Biol. 4, e1000198.
Radman, T., Datta, A., Peterchev, A.V., 2007. In vitro modulation of endogenous rhythms by AC electric fields: syncing with clinical brain stimulation. J. Physiol. 584, 369–370.
Radman, T., Datta, A., Ramos, R.L., Brumberg, J.C., Bikson, M., 2009a. One-dimensional representation of a neuron in a uniform electric field. Conf. Proc. IEEE Eng. Med. Biol. Soc. 2009, 6481–6484.
Radman, T., Ramos, R.L., Brumberg, J.C., Bikson, M., 2009b. Role of cortical cell type and morphology in subthreshold and suprathreshold uniform electric field stimulation in vitro. Brain Stimul. 2, 215–228.
Rahman, A., Reato, D., Arlotti, M., Gasca, F., Datta, A., Parra, L.C., et al., 2013. Cellular effects of acute direct current stimulation: somatic and synaptic terminal effects. J Physiol. 591 (Pt. 10), 2563–2578.
Rall, W., 1959. Branching dendritic trees and motoneuron membrane resistivity. Exp. Neurol. 1, 491–527.
Rall, W., 2011. Core conductor theory and cable properties of neurons. Compr. Physiol. 39–97.
Ranck Jr., J.B., 1975. Which elements are excited in electrical stimulation of mammalian central nervous system: a review. Brain Res. 98, 417–440.
Rattay, F., 1989. Analysis of models for extracellular fiber stimulation. IEEE Trans. Biomed. Eng. 36, 676–682.

Richardson, A.G., McIntyre, C.C., Grill, W.M., 2000. Modelling the effects of electric fields on nerve fibres: influence of the myelin sheath. Med. Biol. Eng. Comp. 38, 438–446.
Richardson, M.J., Melamed, O., Silberberg, G., Gerstner, W., Markram, H., 2005. Short-term synaptic plasticity orchestrates the response of pyramidal cells and interneurons to population bursts. J. Comput. Neurosci. 18, 323–331.
Roth, B.J., 1994. Mechanisms for electrical stimulation of excitable tissue. Crit. Rev. Biomed. Eng. 22, 253–305.
Rubinstein, J.T., 1993. Axon termination conditions for electrical stimulation. IEEE Trans. Biomed. Eng. 40, 654–663.
Salvador, R., Mekonnen, A., Ruffini, G., Miranda, P.C., 2010. Modeling the electric field induced in a high resolution realistic head model during transcranial current stimulation. Conf. Proc. IEEE Eng. Med. Biol. Soc. 2010, 2073–2076.
Salvador, R., Silva, S., Basser, P.J., Miranda, P.C., 2011. Determining which mechanisms lead to activation in the motor cortex: a modeling study of transcranial magnetic stimulation using realistic stimulus waveforms and sulcal geometry. Clin. Neurophysiol. 122, 748–758.
Sasaki, T., Matsuki, N., Ikegaya, Y., 2012. Effects of axonal topology on the somatic modulation of synaptic outputs. J. Neurosci. 32, 2868–2876.
Shu, Y., Hasenstaub, A., Duque, A., Yu, Y., McCormick, D.A., 2006. Modulation of intracortical synaptic potentials by presynaptic somatic membrane potential. Nature 441, 761–765.
Stagg, C.J., Nitsche, M.A., 2011. Physiological basis of transcranial direct current stimulation. Neuroscientist 17, 37–53.
Svirskis, G., Gutman, A., Hounsgaard, J., 1997. Detection of a membrane shunt by DC field polarization during intracellular and whole cell recording. J. Neurophysiol. 77, 579–586.
Svirskis, G., Gutman, A., Hounsgaard, J., 2001. Electrotonic structure of motoneurons in the spinal cord of the turtle: inferences for the mechanisms of bistability. J. Neurophysiol. 85, 391–398.
Tranchina, D., Nicholson, C., 1986. A model for the polarization of neurons by extrinsically applied electric fields. Biophys. J. 50, 1139–1156.
Yi, G.S., Wang, J., Wei, X.L., Tsang, K.M., Chan, W.L., Deng, B., 2014a. Neuronal spike initiation modulated by extracellular electric fields. PLoS One 9, e97481.
Yi, G.S., Wang, J., Wei, X.L., Tsang, K.M., Chan, W.L., Deng, B., et al., 2014b. Exploring how extracellular electric field modulates neuron activity through dynamical analysis of a two-compartment neuron model. J. Comput. Neurosci. 36, 383–399.